Observation of Individual Semiconducting Nanoparticle Collisions by Stochastic Photoelectrochemical Currents

Ashantha Fernando, Suman Parajuli, and Mario A. Alpuche-Aviles*

Department of Chemistry, University of Nevada, Reno, Nevada 89557, United States

Ⓢ *Supporting Information*

ABSTRACT: We describe a method to detect individual semiconducting nanoparticles (NPs) using the photo-electrochemical (PEC) current measured at an ultra-microelectrode (UME). We use photooxidation of MeOH by TiO$_2$ NPs as a model system of photocatalysis in solution. NPs suspended in MeOH under constant illumination produce valence-band holes that oxidize MeOH. The electrons are collected at the UME, and the current-versus-time data show discrete current changes that are assigned to particle-by-particle interactions of the NPs with the UME. The stepwise changes in the photocurrent denote irreversible attachment of NPs to Pt UMEs (<30 μm diameter). We found that accumulation of electrons in the conduction band by the NPs is not enough to explain the stochastic PEC currents. We propose that the observed anodic steps have a PEC nature and are due to photooxidation of MeOH by the NPs at the electrode surface.
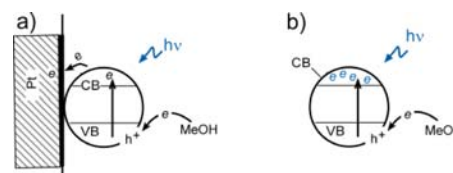
Figure 1. Schematics of (a) photooxidation of MeOH by an NP attached to a Pt UME and (b) accumulation of electrons in the conduction band (CB) of an NP suspended in MeOH.

We present the detection of stochastic photoelectrochemical (PEC) currents due to interactions of individual anatase TiO$_2$ nanoparticles (NPs) with an ultramicroelectrode (UME). Semiconductor nanostructures have been proposed as one of the main avenues to efficiently convert solar energy to electrical[1] or chemical energy.[2] There is interest in nanostructure properties for PEC energy conversion where electron transfer across the semiconductor−liquid interface is key. However, aside from NP synthesis challenges, studying the electrochemical properties of nanometer-sized materials remains complicated because current electroanalytical methods in the nanometer-size domain[3] are still emerging. Here we describe a method to detect the stochastic interactions between suspended semiconductor NPs and a working UME. We measure single-NP PEC currents from NPs under constant illumination. We take our inspiration from the work on electrocatalytic amplification[3e,4] used for collisions of metal NPs with an inert microelectrode. Electrocatalytic amplification has focused on the use of collisions for metal and electrocatalytic NPs with inert UMEs. In this work, the collisions were between illuminated TiO$_2$ NPs and a UME. The electrochemical detection of photogenerated charges in colloidal semiconductors has been demonstrated before,[5] but we are not aware of reports of the detection of individual semiconductor NPs undergoing a photochemical process.

Figure 1 depicts a single NP under illumination in MeOH. Figure 1a shows the injection of electrons into a Pt working electrode by the NP after it is adsorbed on the electrode surface.

The current steps observed in Figure 2a can be explained by interactions between the NP and the UME, with the stepwise current-versus-time (i−t) behavior being indicative of an irreversible interaction.[3e,4d,e] Photooxidation of MeOH also occurs while the NP is suspended (Figure 1b). As reported before, TiO$_2$ NPs suspended in solutions containing a hole (h$^+$) scavenger can be charged by accumulation of electrons in the conduction band (CB).[5,6] NPs suspended in MeOH under our illumination conditions (~15 mW/cm^2 for λ < 400 nm) can be similarly charged, but this electronic charge is not enough to explain the detection of the stochastic steps.

Figure 2 shows our experimental i−t results for NP collisions on a 10 μm diameter Pt UME. The anodic currents are shown as negative. Full experimental details are available in the Supporting Information (SI). Briefly, the colloidal suspension was bubbled with Ar for 30 min. The applied potential was E_{app} = 0.3 V vs I$^-$/I$_3^-$ (10 mM in MeOH) = 0.68 V vs NHE. In our experiments, an aliquot of TiO$_2$ NPs was added to the electrochemical cell to give a final NP concentration of 25 nM; the suspension was dispersed in an ultrasonic bath prior to the PEC experiment (i.e., immediately after the cell was assembled with the Pt UME and the reference and counter electrodes). The Pt UME was prepared in-house using a reported procedure.[7] Under illumination, steps were observed for sample A (18 nm diameter anatase NPs) (Figure 2a). The electrochemical current was in the anodic (negative) direction, indicating that electrons flow from the NPs into the UME. Also, the current steps were not present in the dark (Figure 2b; Figure S4b in the SI shows the trends in the current profile for this control experiment with a different scale). Figure S4 shows the results of additional control experiments performed to investigate the photocatalytic nature of the current steps (see below). The data in Figure 2c show the lack of steps obtained with NPs charged according to ref 6 (sample C, amorphous TiO$_2$).
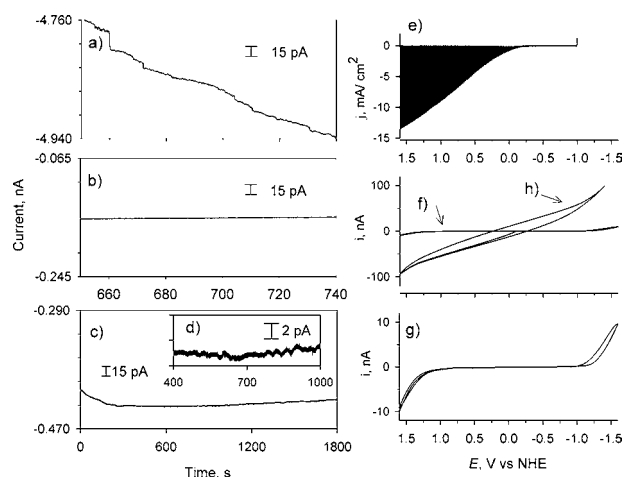
Figure 2. (a) Plot of current vs time for 25 nM anatase NPs suspended in MeOH (sample A) and a 10 μm diameter Pt UME with E_{app} = 0.68 V vs NHE under illumination with a 150 W Xe lamp. (b) As in (a) but in the dark. (c, d) Experiment with charged, blue amorphous TiO_2 NPs (sample C) after charging by continuous illumination for 20 h in 1:1 ethanol/toluene; the inset (d) shows the detail of the current transients. (e) Envelope of a chopped illumination experiment for a film in 0.1 M tetrabutylammonium perchlorate in MeOH [3.5 μm thick anatase film from sample A, scan rate (ν) = 1 mV/s]. (f) CV of the colloidal suspension shown immediately after assembly of the cell; (g) shows the details of the data in (f). (h) CV of the colloid after 3 h of collision experiments (ν = 100 mV/s).

Figure 2e shows the current-versus-potential envelope for a TiO_2 film prepared with sample A. The current was obtained during a linear-sweep scan while the illumination was chopped on and off; the photocurrent onset was at −0.14 V vs NHE. Our E_{app} of 0.68 V vs NHE is more positive than the photocurrent onset, allowing electron injection from the TiO_2 CB onto the Pt UME. Also, the colloid's cyclic voltammogram (CV) in the dark prior to the experiments (Figure 2f,g) showed that there were no Faradaic background processes at E_{app}. The CV prior to the experiments (Figure 2f) is consistent with the CV of neat MeOH (Figure S5; see section III in the SI).

The background current for MeOH oxidation was constant (i < −0.2 nA) at a freshly polished Pt UME (Figure S4c), and the experimental setup under illumination without NPs did not show steps (Figure S4d). No steps were observed for the same concentration of NPs in MeCN under illumination (Figure S4e). MeOH is an efficient h+ scavenger for TiO_2;[8] MeOH is oxidized by valence-band holes, and this generates electrons in the CB that are injected into the Pt UME. We detected steps after illuminating the NP suspension in MeOH but not in MeCN. The stepwise behavior shown in Figure 2a closely resembles the behavior of long-term, irreversible interactions (so-called "sticky" interactions[4d]) that result from stochastic particle-by-particle collisions of an electrocatalyst with an inert UME. In summary, our data indicate that the stochastic photocurrents are due to irreversible NP−electrode interactions that allow detection of photooxidation of MeOH by TiO_2 NPs.

The CV for the TiO_2 suspension in neat MeOH (no supporting electrolyte) run immediately after assembly of the cell (Figure 2f,g) indicates that the iR drop due to the uncompensated resistance (R_u) was negligible at the beginning of the experiment. At longer times (Figure 2h), the iR_u drop increased, most likely because of the accumulation of TiO_2 NPs on the UME surface; both the resistance and the capacitance

increased, and the final value of R_u was estimated to be 15 MΩ using the slope of Figure 2h. We investigated the value of R_u from CVs of ferrocene (Fc) in neat MeOH by simulating them (DigiElch) (Figure S6; see section IV in the SI). On the basis of the CVs for neat MeOH, colloids, and Fc and the digital simulations, R_u at the beginning of the experiments was estimated to be ≪1 MΩ. The charge on the NPs and impurities in the MeOH may have contributed to the conductivity. Interestingly, a TiO_2 film in the dark yielded a well-defined CV without addition of an electrolyte to MeOH (Figure S7).

We studied the stochastic interactions for three different TiO_2 samples (for details, see the SI). Briefly, sample A consisted of anatase TiO_2 NPs grown by a hydrothermal method from an aqueous solution of titanium(IV) isopropoxide (TTIP).[9] The diameter measured by transmission electron microscopy (TEM) was 18 ± 3 nm (Figure S1). No evidence of rutile or other phases was found with powder X-ray diffraction (XRD) (Figure S3a). Electron diffraction confirmed the crystallinity of individual NPs. Sample B containing anatase NPs (Figure S3b) with an average diameter of 70 ± 13 nm (Figure S2) was prepared by suspension of commercial TiO_2 (MKN-TiO_2-A 100, M. K. Impex Corp.). Sample C was a colloidal suspension of amorphous TiO_2 NPs with an average diameter of 15 nm prepared from TTIP in 2-propanol as reported before.[6] Most of the data presented here were obtained with sample A because of its crystallinity and lowest particle size dispersion. Sample B was used to investigate the effect of NP diameter, while sample C was prepared to study the effect of electronic charge.[5,6]

Figure 3a shows $i−t$ data for NP collisions (a different experiment from Figure 2a). In the dark ($t = 0−50$ s), no current
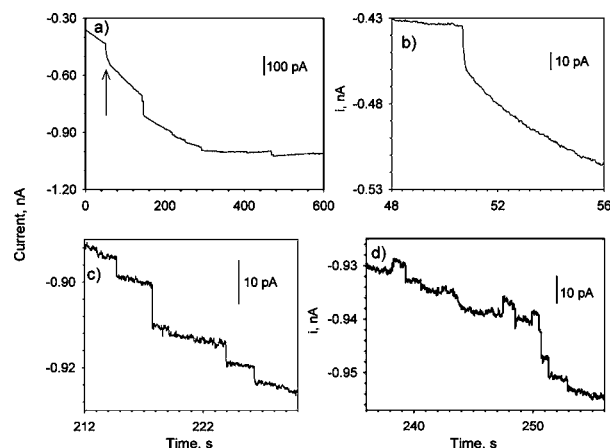
Figure 3. (a) Plot of current vs time for a suspension of 25 nM TiO_2 NPs (sample A) in MeOH and a 10 μm diameter Pt UME with E_{app} = 0.68 V vs NHE illuminated with a 150 W Xe lamp. The arrow shows when the light was turned on. (b−d) Details of the $i−t$ data in (a).

steps were observed, and only a monotonic background was present. In our experiments, the NPs were introduced during the cell setup and could interact with the working electrode before the onset of illumination (denoted by the arrow in Figure 3a). The drift in the current is assigned to the presence of TiO_2 NPs on the Pt surface prior to initial illumination. Immediately after the illumination was turned on, the relatively large transient did not allow the detection of steps (Figure 3b); after the background stabilized (ca. 1 min), current steps were detected (Figure 3c,d). We mostly observed anodic steps (Figure 3c) but

also saw changes in the cathodic direction (Figure 3d), which could be due to NPs leaving the surface or becoming inactive.

The colloidal behavior of NPs in sample A was studied to investigate the possible contributions of individual particles and agglomerates to the observed current steps. Colloidal suspensions were studied with dynamic light scattering (DLS) (see the SI). The DLS data for a TiO$_2$ NP concentration of 25 nM (Figure S8) gave an average particle diameter of 54 ± 20 nm, in contrast to the TEM measurement of 18 ± 3 nm. DLS measurements are biased toward larger particle sizes because the scattering intensity depends with the sixth power of the diameter; therefore, larger NPs are weighted more heavily in the measurement. The final deconvolution of the NP size is shown in Figure S9 (Particle Sizing Systems, Inc.), confirming that most of the NPs in solution were 18 nm in diameter, consistent with the TEM result, with a few (<1%) large NPs with diameters of ca. 120 nm; these larger particles were observed even when the colloid was treated extensively with a sonicating horn.

We also studied the dependence of the PEC behavior on the NP diameter. A suspension of 70 nm diameter anatase NPs was tested (sample B). Figure S10 shows the stochastic events recorded for this sample: current steps were obtained under illumination. Figure 4 shows the statistical distributions of PEC
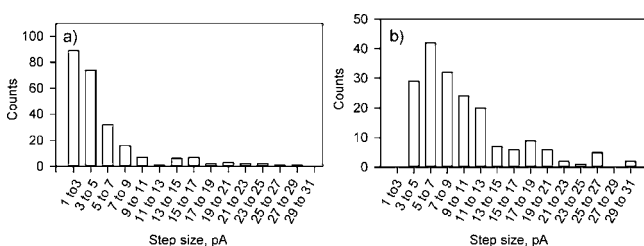
Figure 4. Statistical distributions of PEC steps observed for anatase samples with different diameters: (a) sample A (18 nm diameter), three experiments as in Figure 3; (b) sample B (70 nm diameter), five experiments using an NP concentration of 50 pM with all other experimental conditions as in Figure 3.

steps for a compilation of three experiments for sample A (18 nm diameter; Figure 4a) and five experiments for sample B (70 nm diameter; Figure 4b). For sample A, the average PEC step was 3 pA with a standard deviation of 2 pA. Although currents as high as 60 pA were observed (Figure 3a), most of the steps were less than 8 pA. The observed step frequency (f) was less than that expected for NPs interacting with an electrode at a rate limited by diffusion of the particles (f_p), given by[4d,e]

$$f_p = 4D_{NP}r_dC_{NP}^{bulk} \qquad (1)$$

where D_{NP} is the diffusion coefficient of the suspended NPs, C_{NP}^{bulk} is the NP concentration in solution and r_d is the diameter of the UME. Under our experimental conditions from DLS measurements for sample A, $D_{NP} = 2 \times 10^{-7}$ cm^2/s, $r_d = 5 \times 10^{-4}$ cm, and $C_{NP}^{bulk} = 1.5 \times 10^{13}$ cm^{-3}. Thus, for sample A (18 nm), eq 1 shows that a collision frequency of $f_p^{18\,nm} = 6 \times 10^3$ s^{-1} would be expected if every collision results in detectable adsorption of an NP of average diameter. However, for an NP to produce a current step, the NP must adsorb and also connect with the electrode surface. For sample A, we observed steps with $f = 0.06$ s^{-1} (Figure 4a). For sample B, $f = 0.032$ s^{-1} (section VIII in the SI), which is also lower than that predicted by eq 1. The result that the observed frequencies were lower than those predicted by eq 1 could arise in one of the following ways: (a) The current

steps for sample A could arise from interactions of larger NPs (ca. 120 nm diameter) with the electrode; these NPs would also have a lower collision frequency with the electrode than NPs of average diameter (18 nm). D_{NP} decreases according to the Stokes−Einstein equation, so according to eq 1, f_p is inversely proportional to the NP diameter. Thus, $f^{120\,nm}$ would be a fraction of $f^{18\,nm}$ because of the diameter difference (18/120) and the lower concentration of the 120 nm diameter NPs (1%); eq 1 yields $f_p^{120\,nm} = 9$ s^{-1}, which is closer to the observed value of 0.06 s^{-1}. (b) Alternatively, the observed frequencies could indicate that ca. 1 in 10^5 collisions of NPs of average diameter results in a successful connection between the NP and the UME. For the larger NPs in sample A (120 nm diameter), the ratio would be 1 in 150. An experimental step frequency lower than that predicted by eq 1 for NPs colliding with an electrode is consistent with reports for attachment of metal NPs to electrodes, which found 1 successful event per 10−100 collisions.[4e] However, for semiconductor NPs, the fraction of collisions resulting in a step could be smaller than for metal NPs. Although the expected frequencies for the larger NPs in sample A are closer to the observed step frequencies, this assignment would not be consistent with our finding that for sample B (average diameter of 70 nm), the Gaussian bell was shifted toward higher photocurrents (7 pA; Figure 4b). The distribution for sample B is consistent with a larger photocurrent due to the larger cross section than for the average diameter NP in sample A. The change in the photocurrent was smaller than expected on the basis of the increase in diameter, and this may be due to recombination losses and to the effect of the NP diameter on the probability of collision. It is possible that in sample B we observed the more probable collisions of the smaller NPs (with larger D_{NP}) in the broad diameter distribution shown in Figure S2. Nevertheless, the larger average NP diameter does result in larger photocurrent steps (Figure 4b). To further investigate the effect of the NP diameter on the photocurrent, we need colloids with tunable, monodispersed diameters; we are currently working on these preparations in our laboratory.

The photocurrent dependence on the NP size and the change in the statistical distribution of the photocurrent, in conjunction with the control experiments detailed above, are evidence that the stepwise current observed under illumination is due to interactions of NPs with the UME. NPs in the colloidal suspension interact with the UME to give distinct stochastic electrochemical responses that are consistent with particle-by-particle adsorption onto the electrode.[4e,f] While it is clear that the NPs undergo photocatalytic oxidation of MeOH, we now address in detail the effect of long-term electronic charging on the photocurrent steps. The effect of NP charging has been reported for TiO$_2$ NPs suspended in solutions of hole scavengers.[5,6] Subramanian et al.[6] demonstrated that illuminating the NPs charges the colloid and turns it blue as a result of light absorption by free electrons in the CB. As mentioned above, we prepared these NPs (sample C in 1:1 ethanol/toluene) and confirmed the charging by following the absorption spectra (Figure S11) and the color. However, after continuous illumination for long periods of time (up to 20 h), the NPs turned blue (Figure S14) and in the $i−t$ trace displayed the oscillations shown above (Figure 2c) rather than steps. We also attempted to charge our particles by continuously illuminating them in MeOH, but the electron concentration in our NPs was 250 e$^-$/NP, much smaller than the final charge of 2×10^3 e$^-$/NP estimated in the colloids of sample C reported by Subramanian et al.;[6] we estimated the number of electrons with $\varepsilon = 6235$ M^{-1}

cm^{-1} from ref 6 (Figure S13). Thus, charging alone does not explain the observed stepwise behavior (Figures 2 and 3): the colloids that can accumulate charge strongly (sample C) did not produce photocurrent steps, whereas those that produced steps did not show evidence of charging to same extent as sample C.

Dunn et al.[5a] demonstrated that upon illumination, a TiO$_2$ slurry shows a slow anodic transient that gradually reverses when the illumination is turned off. However, in our experiments, the direction of the background under illumination was not reproducible. While an anodic background (i.e., a low-frequency anodic current) was observed after illumination most of the time (e.g., Figure 3), depending on the history of the electrode we observed a change toward the cathodic direction upon illumination (Figure S15) and slow cathodic drifts in the baseline (Figure S16). Despite these cathodic drifts, the current increased in the anodic direction while the colloid was illuminated. To investigate the effect of charging, we collected data immediately after a period of illumination. Figures S15 and S16 show the data for 18 nm diameter NPs (sample A) and 70 nm diameter NPs (sample B), respectively. Interestingly, we observed current transients in the dark after the illumination was turned off but not before the illumination was turned on (e.g., at the beginning of the experiment). Overall, the transients in the dark observed shortly after the lamp was turned off were less frequent than the steps observed under illumination, but the steps observed for <15 min after the lamp was shut off were similar in magnitude to the most probable steps observed under illumination (Figures S17 and S18, respectively). This suggests that in addition to MeOH photooxidation by NPs, other processes contribute to the current steps observed under illumination.

The smallest well-defined steps we detected under illumination were 1 pA, corresponding to >6 × 10^6 e$^-$/s. Single steps were observed for time scales of 1−2 s or more that correspond to 10^6 electrons stored in a single NP of sample A. As mentioned earlier, the maximum number of electrons we were able to charge was 250 e$^-$/NP after illuminating sample A for 2 h in MeOH. This long-term charging in the CB was negligible with respect to the number of electrons we collected during single photocurrent steps under illumination or after the illumination was turned off. The large number of electrons detected in a current step is indicative that these current steps are not due to electrons accumulated in the CB by the NPs while suspended in MeOH. We propose that the steps are due to electrons flowing through the NP while the particle is connected with the UME surface. The photocatalytic oxidation of MeOH is likely the main process that produces these electrons. We note that the magnitude of the current steps is too large for the number of photons absorbed by an NP, as estimated from the lamp manufacturer's data (~15 mW/cm^2 for λ < 400 nm) and the NP geometric cross section (see the Experimental Section in the SI). We are currently investigating the photon collection efficiency and will report our findings in due time. Another factor under investigation is the contribution from intermediates of byproducts of the photo-oxidation of MeOH. As a result of the PEC oxidation of MeOH at E_{app} = 0.68 V vs NHE, CO and other carbon species could be produced at the Pt surface (for details, see the SI), and these intermediates could be photooxidized by the NPs upon making contact with the electrode surface.[10] Also, after the illumination is turned off, intermediates or byproducts could be detected at the electrode surface if the surface becomes available when NPs leave the surface; this Faradaic process may contribute to the current detected under illumination. This could account for the current under illumination being dependent on the history of the

electrode surface and could explain the current steps observed in the dark shortly after illumination.

In conclusion, we have described a method to detect individual semiconducting NPs in a colloid as they interact with a working Pt UME. As a proof of concept, we studied anatase TiO$_2$ NPs suspended in MeOH. The stepwise behavior of the photocurrent denotes long-term interactions of NPs with the UME, particle-by-particle. Overall, long-term charging by electrons in the CB does not explain the observed step magnitude. Studies of the mechanism whereby photogenerated electrons are produced by TiO$_2$ NPs connected to the Pt surface (e.g., Figure 1a), including possible contributions of photogenerated intermediates or byproducts, are currently underway.

■ ASSOCIATED CONTENT

ⓢ Supporting Information
Experimental section and additional data. This material is available free of charge via the Internet at http://pubs.acs.org.

■ AUTHOR INFORMATION

Corresponding Author
malpuche@unr.edu

Notes
The authors declare no competing financial interest.

■ REFERENCES
(1) O'Regan, B.; Grätzel, M. *Nature* **1991**, *353*, 737.
(2) (a) Sivula, K.; Zboril, R.; Le Formal, F.; Robert, R.; Weidenkaff, A.; Tucek, J.; Frydrych, J.; Grätzel, M. *J. Am. Chem. Soc.* **2010**, *132*, 7436. (b) Brimblecombe, R.; Koo, A.; Dismukes, G. C.; Swiegers, G. F.; Spiccia, L. *J. Am. Chem. Soc.* **2010**, *132*, 2892. (c) Song, W.; Brennaman, M. K.; Concepcion, J. J.; Jurss, J. W.; Hoertz, P. G.; Luo, H.; Chen, C.; Hanson, K.; Meyer, T. J. *J. Phys. Chem. C* **2011**, *115*, 7081.
(3) (a) Fan, F.-R. F.; Bard, A. J. *Nano Lett.* **2008**, *8*, 1746. (b) Myung, N.; Ding, Z.; Bard, A. J. *Nano Lett.* **2002**, *2*, 1315. (c) Myung, N.; Lu, X.; Johnston, K. P.; Bard, A. J. *Nano Lett.* **2004**, *4*, 183. (d) Tel-Vered, R.; Bard, A. J. *J. Phys. Chem. B* **2006**, *110*, 25279. (e) Xiao, X.; Bard, A. J. *J. Am. Chem. Soc.* **2007**, *129*, 9610.
(4) (a) Bard, A. J.; Zhou, H.; Kwon, S. J. *Isr. J. Chem.* **2010**, *50*, 267. (b) Kwon, S. J.; Bard, A. J. *J. Am. Chem. Soc.* **2012**, *134*, 7102. (c) Kwon, S. J.; Fan, F.-R. F.; Bard, A. J. *J. Am. Chem. Soc.* **2010**, *132*, 13165. (d) Kwon, S. J.; Zhou, H.; Fan, F.-R. F.; Vorobyev, V.; Zhang, B.; Bard, A. J. *Phys. Chem. Chem. Phys.* **2011**, *13*, 5394. (e) Xiao, X.; Fan, F.-R. F.; Zhou, J.; Bard, A. J. *J. Am. Chem. Soc.* **2008**, *130*, 16669. (f) Zhou, H.; Fan, F.-R. F.; Bard, A. J. *J. Phys. Chem. Lett.* **2010**, *1*, 2671.
(5) (a) Dunn, W. W.; Aikawa, Y.; Bard, A. J. *J. Am. Chem. Soc.* **1981**, *103*, 3456. (b) Ward, M. D.; Bard, A. J. *J. Phys. Chem.* **1982**, *86*, 3599. (c) Dunn, W. W.; Aikawa, Y.; Bard, A. J. *J. Electrochem. Soc.* **1981**, *128*, 222.
(6) Subramanian, V.; Wolf, E. E.; Kamat, P. V. *J. Am. Chem. Soc.* **2004**, *126*, 4943.
(7) Wightman, R. M.; Wipf, D. O. *Electroanal. Chem.* **1989**, *15*, 267.
(8) Yoneyama, H.; Toyoguchi, Y.; Tamura, H. *J. Phys. Chem.* **1972**, *76*, 3460.
(9) Zaban, A.; Ferrere, S.; Sprague, J.; Gregg, B. A. *J. Phys. Chem. B* **1997**, *101*, 55.
(10) Korzeniewski, C.; Childers, C. L. *J. Phys. Chem. B* **1998**, *102*, 489.